nature

LETTERS

Conformational changes in an ultrafast light-driven enzyme determine catalytic activity

Olga A. Sytina[1], Derren J. Heyes[2], C. Neil Hunter[3], Maxime T. Alexandre[1], Ivo H. M. van Stokkum[1], Rienk van Grondelle[1] & Marie Louise Groot[1]

The role of conformational changes in explaining the huge catalytic power of enzymes is currently one of the most challenging questions in biology[1–7]. Although it is now widely regarded that enzymes modulate reaction rates by means of short- and long-range protein motions[3–7], it is almost impossible to distinguish between conformational changes and catalysis. We have solved this problem using the chlorophyll biosynthetic enzyme NADPH:protochlorophyllide (Pchlide) oxidoreductase, which catalyses a unique light-driven reaction involving hydride and proton transfers[8]. Here we report that prior excitation of the enzyme-substrate complex with a laser pulse induces a more favourable conformation of the active site, enabling the coupled hydride and proton transfer reactions to occur. This effect, which is triggered during the Pchlide excited-state lifetime and persists on a long timescale, switches the enzyme into an active state characterized by a high rate and quantum yield of formation of a catalytic intermediate. The corresponding spectral changes in the mid-infrared following the absorption of one photon reveal significant conformational changes in the enzyme, illustrating the importance of flexibility and dynamics in the structure of enzymes for their function.

Dehydrogenase enzymes catalyse proton and hydride transfer reactions with rate enhancements of up to 10^{17} in comparison with the equivalent reaction in solution[1]. However, understanding the role of conformational changes in this catalytic power is challenging, as the hydrogen transfer processes are much faster than the structural changes associated with switching of an enzyme from an 'inactive' to an 'active' conformation[9–11].

Here we study an enzyme from the family of alcohol dehydrogenases, NADPH:protochlorophyllide oxidoreductase (POR), which has provided a unique opportunity to observe the light-driven formation of an activated enzyme conformation before catalysis. The requirement of light for initiation of catalysis by POR makes it an excellent model system for studying the mechanism and timescales of enzymatic proton and hydride transfers, as the enzyme-substrate complex can be pre-formed in the dark and catalysis initiated by a short pulse of light[8]. POR catalyses the *trans* addition of hydrogen from NADPH across the C17–C18 double bond of the D ring of Pchlide to produce chlorophyllide (Chlide)[12], which is an important regulatory step for chlorophyll biosynthesis and the subsequent assembly of the photosynthetic apparatus[8,12,13]. It is proposed that a conserved Tyr residue donates a proton to the C18 position[14] and a hydride is transferred from the *proS* face of the NADPH nicotinamide ring to the C17 position of the Pchlide molecule[15,16] (Fig. 1). The involvement of the Pchlide excited state in the reduction suggests that significant parts of the reaction may occur on the picosecond timescale. Indeed, we have previously shown that catalysis can be

triggered with a 50-fs laser pulse, and, using ultrafast pump–probe absorption spectroscopy, observed that the formation of a reaction intermediate in the excited state proceeds with time constants of 3 ps and 400 ps (ref. 17). In addition, following the formation of the POR–Chlide–NADP$^+$ state there is a series of ordered product release and cofactor binding events in which domain movements and/or reorganization of the protein have an important role[18–21].

Here we use ultrafast pump–probe absorption difference spectroscopy to study the initial catalytic steps in more detail, which reveals that a critical light-driven activation of the enzyme is required before catalysis. The use of a Lissajous sample scanner in combination with very high detection sensitivity facilitates quantitative measurements under single-pulse conditions, allowing us to measure reaction rates and quantum yields as functions of the total number of laser shots previously seen by the sample. Our spectrometer ensures that in each scan the sample is illuminated by only one shot of the laser, with an excitation density of ~ 0.03 absorbed photons per enzyme-substrate complex. The time-dependent absorption difference spectra obtained after a laser pulse are shown in Fig. 2 for a number of subsequent scans in the form of evolution-associated-difference spectra (EADS). The EADS result from a global analysis of the data in which the time-dependent behaviour of the absorption difference spectra is fitted to three exponentials that evolve in a sequential manner, $A \rightarrow B \rightarrow C \rightarrow$, with increasing lifetimes τ_1, τ_2 and τ_3. The
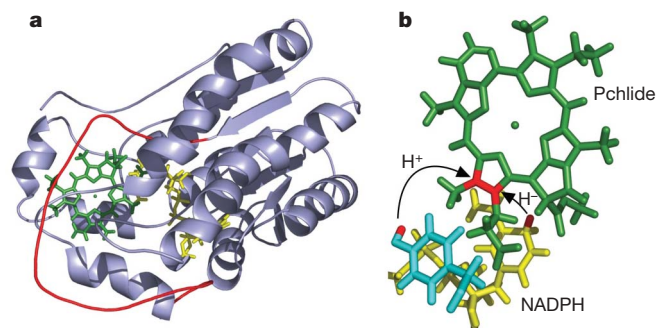

Figure 1 | Homology model of POR from *Synechocystis*[24]. a, The structure consists of a central parallel β-sheet comprising seven β-strands, surrounded by nine α-helices. The 33-residue insertion (red) is unique to POR, and is proposed to be involved in Pchlide (green) binding. **b**, Three-dimensional model of the POR-catalysed reaction based on the structural homology model of POR[24] and the proposed mechanism of hydride and proton transfers[14]. The proton at the C18 position of Pchlide is derived from Tyr 189 (numbering in *Synechocystis* POR, cyan) and the hydride transferred to the C17 position is derived from the *proS* face of NADPH (yellow).

---

[1]Department of Physics and Astronomy, Faculty of Sciences, Vrije Universiteit, De Boelelaan 1081, 1081 HV Amsterdam, The Netherlands. [2]Manchester Interdisciplinary Biocentre, University of Manchester, 131 Princess Street, Manchester M1 7DN, UK. [3]Department of Molecular Biology and Biotechnology, University of Sheffield, Firth Court, Western Bank, Sheffield S10 2TN, UK.

EADS represent the spectra of the states A, B and C. Inspection of the absorption difference spectra shows that, although the enzyme shows spectral evolution on an ultrafast timescale, it is clear that prior exposure to light has a marked influence on the dynamics and, more profoundly, the yield of the reaction.

All scans show a negative band that peaks at 640 nm and originates in the laser-excited, enzyme-bound Pchlide substrate. However, in the later scans a significant negative band also appears at ~675 nm, owing to a Chlide-precursor species formed in its excited state (Fig. 2b, c)[17]. Recent theoretical studies[22] together with preliminary experimental data (Supplementary Fig. 1) suggest that this precursor species (I_{675}^*) is likely to represent a state in which Pchlide forms a strongly hydrogen-bonded complex with residues in its direct environment and/or NADPH, which is essential for the subsequent hydride and proton transfer steps to proceed on a microsecond time-scale. In the initial scans there is a progressive blue shift of the signal at 640 nm, in combination with a loss of stimulated emission at the red end of this band (Fig. 2a), and only a very small amount of negative signal at ~675 nm is formed in 700 ps. The formation time and yield of the negative 675-nm signal, indicative of the I_{675}^* precursor, is completely dependent upon the scan number; in later scans I_{675}^* formation occurs with 4-ps and 500-ps time constants and with a much higher yield (Fig. 2c). In addition, direct excitation of the Chlide product, formed during previous scans, is observed in the later scans, as the signal at ~670 nm is negative in the time-zero spectra (black spectra in Fig. 2b, c).
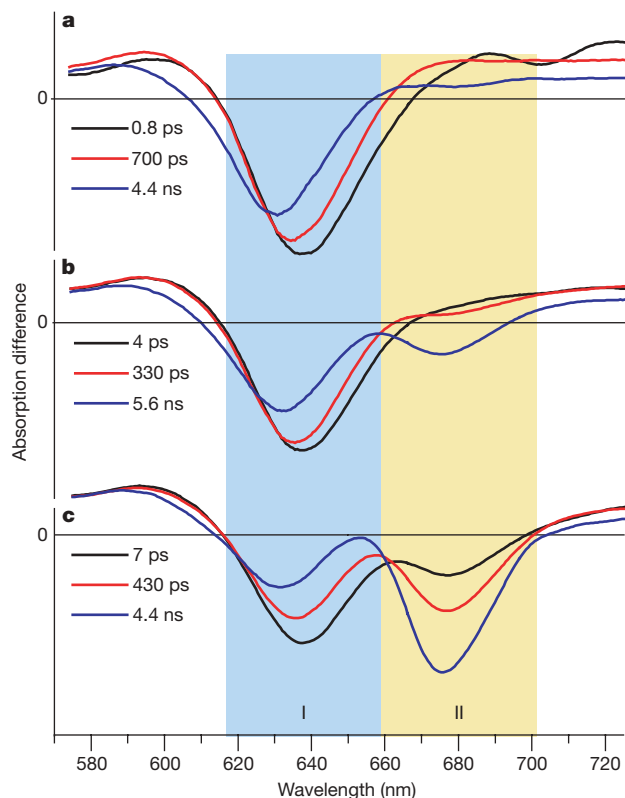

Figure 2 | Evolution-associated difference spectra resulting from a global analysis, as a function of illumination time. A sequential model with increasing lifetimes was used. Excitation of the POR–Pchlide–NADPH enzyme-substrate complex was at 475 nm (using a 50-fs laser pulse[25]), the induced absorption changes were recorded at 48 different time points between −10 ps and 5 ns, and one spectrum consists of 256 spectral points. Region I is composed of bleached absorption and stimulated emission from the Pchlide substrate, and in region II the stimulated emission signal is observed from the I_{675}^* product formed in the excited state. **a**, Scans 1 and 2; **b**, scans 6–12; **c**, scans 26–55. The vertical scale corresponds to an absorption change of -30×10^{-3}.
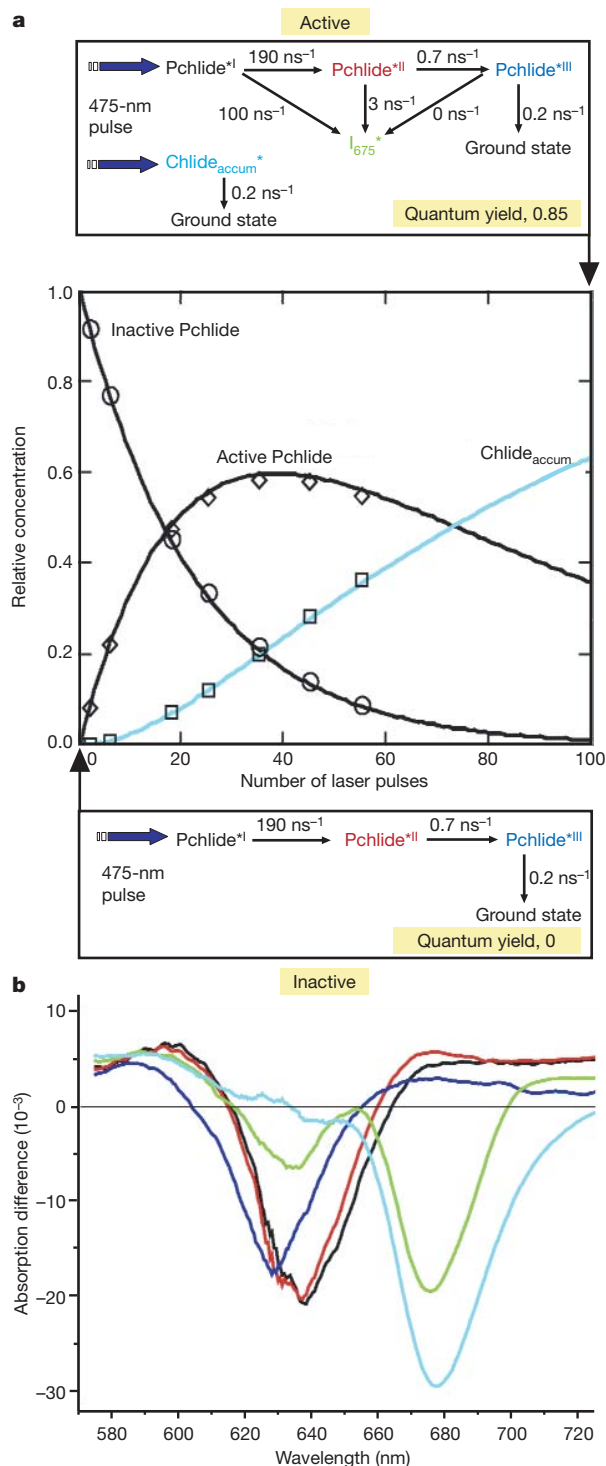

Figure 3 | Target analysis[26] of the illumination-dependent POR pump–probe data sets. a, Model for the ultrafast catalytic reactions in POR: kinetic scheme for active enzymes that can form the photoproduct I_{675}^* (top); concentration of active (diamonds) and inactive (circles) enzymes and accumulated Chlide (squares) as a function of applied laser pulse (middle); kinetic scheme for inactive enzymes, showing only Pchlide* photochemistry (from Pchlide*[I] to Pchlide*[II] to Pchlide*[III]) (bottom). The concentrations at $t = 0$ of inactive and active enzymes and Chlide accumulated in previous scans (Chlide$_{accum}$*) are assumed to follow the populations of unexcited, singly excited and twice-excited enzymes, respectively (solid lines drawn for an excitation density of 0.045/pulse). **b**, Species-associated difference spectra of POR of the Pchlide*[I], Pchlide*[II], Pchlide*[III], I_{675}^* and Chlide$_{accum}$* states obtained from the target analysis; the spectra are colour coded to match the states in **a**.

To analyse the data in more detail, we fit the full set of spectra to a minimal model (Fig. 3a). In this model we divide the POR enzyme population into an 'inactive' fraction, which describes the Pchlide* dynamics (between the states denoted Pchlide*^{I}, Pchlide*^{II} and Pchlide*^{III}, in that order), and an 'active' fraction, in which there is an additional reaction path from each of the Pchlide*^{I}, Pchlide*^{II} and Pchlide*^{III} states to I$_{675}$*. Also, the directly excited Chlide formed in previous scans is included. The results of this target analysis are shown in Fig. 3, and representative traces and fits can be found in the Supplementary Information.

The size of the fraction of active enzyme is dependent on the number of laser pulses and increases in a similar manner to the proportion of enzymes that have been excited at least once. In fully light-activated enzymes, the quantum yield of transformation of Pchlide to the Chlide precursor I$_{675}$* is 0.85, of which 0.35 occurs by means of the single-step mechanism, with an effective rate of $\sim$300 ns^{-1} (Fig. 3a), and 0.5 by means of the two-step mechanism, with an effective rate of 3.7 ns^{-1}. Also, the accumulating concentration of Chlide (Fig. 3a, cyan curve) can be described with a yield of 0.3 for the I$_{675}$*-to-Chlide reaction, consistent with previous quantum yield measurements of 0.21 (ref. 18). Because we exclude any possible effects of temperature or changing sample conditions during each scan (Supplementary Fig. 2), there must be a direct relationship between the rate of the reaction and the level of illumination, in terms of the number of laser pulses used for prior activation of the enzyme-substrate complexes. Therefore, it appears that catalysis cannot proceed until the enzyme-substrate complex has been excited at least once, suggesting that the first photon turns the enzyme 'on', whereas the second photon induces catalysis. Additional experiments, in which we place an activated enzyme sample in the dark for several periods of time, reveal that the active conformation persists for at least 19 hours (Supplementary Fig. 4), suggesting that the enzyme-substrate complex has a 'memory' which lasts for a long time relative to the timescale of the catalytic events. In addition, we also show that, upon completion of a single turnover and mixing with fresh Pchlide, POR retains between 80 and 100% of its catalytic activity (Supplementary Fig. 5).

These results demonstrate that the rate and quantum yield of formation of the intermediate state I$_{675}$* is significantly enhanced after the Pchlide substrate has cycled through the excited state at least once. This effect may arise from a more favourable catalytic configuration of the enzyme-substrate complex, caused by the changed electron distribution in the Pchlide excited state. To investigate whether conformational changes in the enzyme are induced upon the absorption of a photon, we recorded absorption difference spectra in the mid-infrared region under illumination conditions similar to those used in Fig. 3. The difference spectra (light-induced minus dark) are recorded every second using a Fourier transform infrared (FTIR) spectrometer in rapid-scan mode, while flashing with 5-ns laser pulses at a 20-Hz repetition rate to excite the enzyme-substrate complex. The traces recorded between 1,800 and 1,250 cm^{-1} (Fig. 4a) clearly show different saturation behaviours at different frequencies, suggesting the occurrence of two or more different light-induced processes. The time- or photon-flux-dependent behaviour of the data can be described with a sequential model, A $\rightarrow$ B $\rightarrow$ C $\rightarrow$, with increasing lifetimes/photon fluxes τ_1, τ_2 and τ_3, resulting in the spectra depicted in Fig. 4b. The presence of relatively large signals in the amide I and II regions shows that brief illumination of the enzyme-substrate complex (corresponding to 20 flashes of 5-ns laser pulses) yields conformational changes in the secondary structure of the enzyme. The amplitude of these signals is increased by further illumination of the sample (Fig. 4b, red spectrum), and the conformational change in POR has an extremely long lifetime of many minutes (Supplementary Fig. 6). However, in neither case are these signals accompanied by catalytic activity; only continued illumination produces the mid-infrared signatures for the disappearance of Pchlide and NADPH and the formation of Chlide and NADP$^+$ (Fig. 4b, blue spectrum).

The two distinct phases in the mid-infrared spectral evolution clearly indicate that the enzyme undergoes two separate processes upon illumination: there is an initial structural optimization, and then—only after continued illumination—is Pchlide converted into Chlide. Combining the results from the femtosecond visible pump–probe and those in the mid-infrared, we conclude that absorption of the first photon activates the enzyme, which results in a high quantum yield formation of I$_{675}$* on the picosecond timescale when a second photon is absorbed. The structural changes are currently difficult to quantify using the spectroscopic changes in the infrared, and may involve minor structural rearrangements, optimizing the alignment of the NADPH-nicotinamide ring and the Tyr residue with the D ring of Pchlide to increase the rate of the hydride and proton transfers. On the other hand, the long lifetime and the fact that activation is not reversed upon turnover of the enzyme may suggest an irreversible process in the POR protein. It would appear that the conformational change is both highly efficient (that is, it needs only one photon) and very specific, resulting in a high catalytic
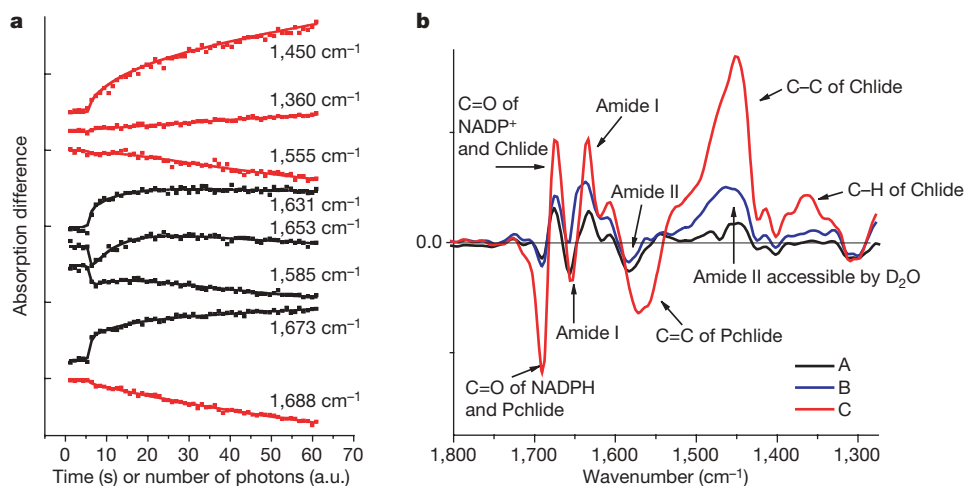

Figure 4 | Mid-infrared absorption difference data. a, Selected time/photon flux traces; **b,** corresponding evolution-associated difference spectra. The EADS result from a global analysis of the light-induced minus dark difference spectra using a sequential model with increasing lifetimes, A $\rightarrow$ B $\rightarrow$ C. Negative bands arise from the disappearance of infrared absorption associated with Pchlide and NADPH substrates and the POR protein in the dark state, and positive bands are due to the appearance of new species in the reaction upon illumination, such as Chlide, NADP$^+$ and POR in its active conformation. a.u., arbitrary units.

quantum yield. It is likely that such a directional conformational change underlies efficient hydrogen and proton transfers in many other enzymes.

Several other enzymes have been found to have a 'rest' conformation and a second conformation in which the enzyme is 'active'[9,10,23]. In POR, however, we find that the active conformation is retained during and after turnover. This light-adaptation of POR may have an important role in green plants and other photosynthetic organisms, as it allows the enzyme to capitalize on very low or erratic photon fluxes by remaining in an activated, catalytically efficient state for long periods.

METHODS SUMMARY

Composition of the samples. POR from the cyanobacterium *Thermosynechococcus elongatus* BP-1 was produced as previously described[18]. The samples contained 0.5 mM Pchlide, 0.5 mM POR and 2.5 mM NADPH in activity buffer (50 mM Tris (pH 7.5), 100 mM NaCl, 1% Genapol, 0.1% β-mercaptoethanol) and were kept in the dark at all times. For FTIR spectroscopy experiments the H_2O in the buffer was replaced by D_2O.

Visible pump–probe experiments. Absorption difference spectra at 48 different time points between −10 ps and 5 ns were collected with a set-up based on a 1-kHz amplified laser system, described in more detail in the Methods. The collection of each data set took 40 s, during which each part of the sample was illuminated by a single shot of the laser. Hence, in subsequent scans the sample was illuminated by more laser pulses.

Target analysis. A full description of the target analysis is given in the Methods.

FTIR spectroscopy experiments. Light-induced minus dark difference spectra were measured by means of an FTIR Bruker IFS 66/S spectrometer in rapid-scan mode. First we collected infrared steady-state absorption spectra of the POR–NADPH–Pchlide complex in the dark, as the background, and then we recorded the induced absorption changes every second while the whole area of the sample cell was excited at 444 nm by the 20-Hz output of a Continuum Panther optical parametric oscillator pumped by a Continuum Surelite I-20 Nd:YAG laser.

Full Methods and any associated references are available in the online version of the paper at www.nature.com/nature.

1. Benkovic, S. J. & Hammes-Schiffer, S. A perspective on enzyme catalysis. *Science* **301**, 1196–1202 (2003).
2. Villà, J. & Warshel, A. Energetics and dynamics of enzymatic reactions. *J. Phys. Chem. B* **105**, 7887–7907 (2001).
3. Masgrau, L. *et al.* Atomic description of an enzyme reaction dominated by proton tunneling. *Science* **312**, 237–241 (2006).
4. Kohen, A., Cannio, R., Bartolucci, S. & Klinman, J. P. Enzyme dynamics and hydrogen tunnelling in a thermophilic alcohol dehydrogenase. *Nature* **399**, 496–499 (1999).
5. Eisenmesser, E. Z. *et al.* Intrinsic dynamics of an enzyme underlies catalysis. *Nature* **438**, 117–121 (2005).
6. Agarwal, P. K. Role of protein dynamics in reaction rate enhancement by enzymes. *J. Am. Chem. Soc.* **127**, 15248–15256 (2005).
7. Wang, L., Goodey, N. M., Benkovic, S. J. & Kohen, A. Coordinated effects of distal mutations on environmentally coupled tunneling in dihydrofolate reductase. *Proc. Natl Acad. Sci. USA* **103**, 15753–15758 (2006).
8. Heyes, D. J. & Hunter, C. N. Making light work of enzyme catalysis: protochlorophyllide oxidoreductase. *Trends Biochem. Sci.* **30**, 642–649 (2005).
9. Eisenmesser, E. Z., Bosco, D. A., Akke, M. & Kern, D. Enzyme dynamics during catalysis. *Science* **295**, 1520–1523 (2002).
10. Flomenbom, O. *et al.* Stretched exponential decay and correlations in the catalytic activity of fluctuating single lipase molecules. *Proc. Natl Acad. Sci. USA* **102**, 2368–2372 (2005).
11. Boehr, D. D., McElheny, D., Dyson, H. J. & Wright, P. E. The dynamic energy landscape of dihydrofolate reductase catalysis. *Science* **313**, 1638–1642 (2006).
12. Lebedev, N. & Timko, M. P. Protochlorophyllide photoreduction. *Photosyn. Res.* **58**, 5–23 (1998).
13. Griffiths, W. T. Reconstruction of chlorophyllide formation by isolated etioplast membranes. *Biochem. J.* **174**, 681–692 (1978).
14. Wilks, H. M. & Timko, M. P. A light-dependent complementation system for analysis of NADPH:protochlorophyllide oxidoreductase. Identification and mutagenesis of two conserved residues that are essential for enzyme activity. *Proc. Natl Acad. Sci. USA* **92**, 724–728 (1995).
15. Valera, V., Fung, M., Wessler, A. N. & Richards, W. R. Synthesis of 4R- and 4S-tritium labeled NADPH for the determination of the coenzyme stereospecificity of NADPH-protochlorophyllide oxidoreductase. *Biochem. Biophys. Res. Commun.* **148**, 515–520 (1987).
16. Begley, T. P. & Young, H. Protochlorophyllide reductase. 1. Determination of the regiochemistry and the stereochemistry of the reduction of protochlorophyllide to chlorophyllide. *J. Am. Chem. Soc.* **111**, 3095–3096 (1989).
17. Heyes, D. J., Hunter, C. N., van Stokkum, I. H. M., van Grondelle, R. & Groot, M. L. Ultrafast enzymatic reaction dynamics in protochlorophyllide oxidoreductase. *Nature Struct. Biol.* **10**, 491–492 (2003).
18. Heyes, D. J., Ruban, A. V., Wilks, H. M. & Hunter, C. N. Enzymology below 200K: the kinetics and thermodynamics of the photochemistry catalysed by protochlorophyllide oxidoreductase. *Proc. Natl Acad. Sci. USA* **99**, 11145–11150 (2002).
19. Heyes, D. J. & Hunter, C. N. Identification and characterization of the product release steps within the catalytic cycle of protochlorophyllide oxidoreductase. *Biochemistry* **43**, 8265–8271 (2004).
20. Heyes, D. J. *et al.* The first catalytic step of the light-driven enzyme protochlorophyllide oxidoreductase proceeds via a charge transfer complex. *J. Biol. Chem.* **281**, 26847–26853 (2006).
21. Heyes, D. J., Ruban, A. V. & Hunter, C. N. protochlorophyllide oxidoreductase: 'Dark' reactions of a light-driven enzyme. *Biochemistry* **42**, 523–528 (2003).
22. Zhao, G.-J. & Han, K.-L. Site-specific solvation of the photoexcited protochlorophyllide *a* in methanol: formation of the hydrogen-bonded intermediate state induced by hydrogen-bond strengthening. *Biophys. J.* **94**, 38–46 (2008).
23. Lu, H. P., Xun, L. & Xie, X. S. Single-molecule enzymatic dynamics. *Science* **282**, 1877–1882 (1998).
24. Townley, H. E., Sessions, R. B., Clarke, A. R., Dafforn, T. R. & Griffiths, W. T. Protochlorophyllide oxidoreductase: A homology model examined by site-directed mutagenesis. *Proteins* **44**, 329–335 (2001).
25. Groot, M. L., Breton, J., van Wilderen, L. J. G. W., Dekker, J. P. & van Grondelle, R. Femtosecond visible/visible and visible/mid-IR pump-probe study of the photosystem II core antenna complex CP47. *J. Phys. Chem. B* **108**, 8001–8006 (2004).
26. van Stokkum, I. H. M., Larsen, D. S. & van Grondelle, R. Global and target analysis of time-resolved spectra. *Biochim. Biophys. Acta* **1657**, 82–104 (2004).

Author Contributions O.A.S., D.J.H., M.T.A. and M.L.G. produced the samples and performed all of the experiments. O.A.S., I.H.M.v.S. and M.L.G. analysed the data. D.J.H., C.N.H., R.v.G. and M.L.G. coordinated the study, designed the experiments and wrote the paper. All authors discussed the results and commented on the manuscript.

Author Information Reprints and permissions information is available at www.nature.com/reprints. Correspondence and requests for materials should be addressed to C.N.H. (c.n.hunter@sheffield.ac.uk).

METHODS

Ultrafast pump–probe spectroscopy. The laser set-up has been described previously[25]. Briefly, the output of a regenerative Ti:sapphire amplifier operating at 1 kHz (Hurricane, Spectra Physics), producing 85-fs pulses of ~0.8 mJ, was used to pump a non-collinear optical amplifier. This amplifier was tuned to 475 nm to excite the complexes at the red edge of the Soret band (S0 → S2 transition) of Pchlide, where the absorption of the product Chlide is minimal. The excitation energy per laser flash was 100 nJ, focused to a spot of about 150-μm diameter. A small part of the 800-nm output was used to generate a white light continuum in a sapphire plate and, after interrogating the sample, was dispersed in a spectrograph and detected on a 256-element diode array read out at 1 kHz. Detection was in the wavelength region 600–700 nm, probing the S0 ↔ S1 transition of Pchlide and products. The polarization of the probe light was at the 'magic angle' (54.7°) with respect to the excitation light. The instrument response function was about 130 fs. The sample was put in a CaF_2 cell of 200-μm path length, contained in a Lissajous sample scanner. The scanner was moved at such speed that a new part of the sample was illuminated at every shot (the shots taken at the corners of the scanned area, where the scanner velocity is lower, were discarded). The same volume was illuminated again after 1–2 min. One scan of the pump-delay line, recording data from −15 ps to 6 ns, took ~40 s, so each scan corresponds to one laser pulse with an energy density of ~0.03 photons per enzyme. Previous ultrafast transient absorption measurements on POR have used a flow cell for the sample (~4 ml) and the acquisition time of one scan was approximately 10 min (ref. 11). All experiments were performed at room temperature (22 °C). The data was analysed using a global fit algorithm[25]. The spectra shown in Fig. 2 are the averages of spectra recorded on three freshly prepared samples.

Temperature effects. A simple calculation shows that negligible water heating occurs in our experiment. If we suppose that half of the laser energy ($E = 100$ nJ) is absorbed by the sample, it can be calculated that with a volume of 0.1 ml (the water thermal capacity being $4\,J\,ml^{-1}\,K^{-1}$), we would need 8×10^6 laser shots to heat the water by 1 K, which at 500 Hz takes 4 h. This is neglecting thermalization with the environment. In a similar way, we can calculate with convection equations that if the sample is at 5 °C when it is put into the cell, it takes only about 77 s to reach room temperature. Thus, we may consider the enzymes to be at room temperature during the experiments.

FTIR spectroscopy experiments. The infrared absorption difference signals in the frequency range 1,660–1,630 cm^{-1} can be assigned to the amide I protein band[27] and the bleaches of absorption at both 1,580 cm^{-1} and at 1,470 cm^{-1} to amide II[28], the former representing amide groups not accessible by D_2O and the latter representing amide groups that are accessible by the solvent. Differential bands between 1,690 and 1,670 cm^{-1} were assigned to carbonyl vibrations of $NADPH/NADP^+$ (ref. 28) and Pchlide/Chlide[29–31]. The 1,570–1,450 cm^{-1} differential signal is assigned to the Pchlide-to-Chlide conversion process representing disappearance of a C=C mode and appearance of a C–C mode[29–31]. The signal around 1,360 cm^{-1} was assigned to the appearance of a chlorin C–H mode[29–31], and therefore signals formation of Chlide.

Global analysis. For each illumination condition, all 48 time-gated spectra (measured at 256 wavelengths) were collated in a matrix, which was globally fitted using a sequential kinetic scheme with increasing lifetimes[26]. From this the lifetimes and the EADS were estimated. The quality of the fit was judged by inspection of the singular vectors of the matrix of residuals, which had to be structureless. The instrument response function was described by a Gaussian shape, and the white-light dispersion over the spectral range was modelled as a second-order polynomial. With increasing lifetimes, and thus decreasing rates, the first of the EADS decays with the first lifetime and corresponds to the difference spectrum at time zero with an ideal, infinitely small instrument response function. The second of the EADS is formed with the first lifetime and decays with the second lifetime. The third of the EADS (and in our case the final one) represents the difference spectrum of the longest-living species. It is formed with the second lifetime and decays with the third lifetime. The error in the lifetimes obtained from the fitting procedure does not exceed 10%. EADS may not represent pure species, and they are interpreted as a weighted sum (with only positive contributions) of species-associated difference spectra (SADS). Referring to Fig. 2, we note that in the blue spectral region (612–656 nm) an evolution of the Pchlide* bleaching and stimulated emission is observed, whereas in the red spectral region (656–700 nm) Pchlide* excited-state absorption, as well as Chlide* bleaching and stimulated emission, contributes.

Target analysis. To resolve the SADS from the EADS, a target analysis was performed simultaneously on data from all seven illumination conditions (~98,000 data points in total). In this target analysis, the kinetic scheme from Fig. 3a was used to estimate the microscopic rate constants and SADS of the three

successive Pchlide* species (black, red and blue), the accumulated Chlide* (Chlide$_{accum}$*, cyan) bleaching and stimulated emission, and the stimulated emission of the I$_{675}$* product (green). We assume that the Pchlide* photochemistry is intrinsic for Pchlide* and therefore independent of the activation state of the protein.

The concentrations of inactive and active enzymes and of Chlide$_{accum}$* at $t = 0$ for each successive scan are assumed to depend on the number of applied laser pulses according to the analytical expression for the concentration of unexcited, singly excited and twice-excited enzymes obtained by solving the coupled differential equations belonging to the following rate equation:

$$\text{inactive} \xrightarrow{e_1} \text{active} \xrightarrow{e_2} (\text{I}_{675}{}^*)\ \text{Chlide}$$
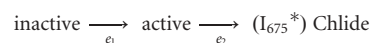
Here e_1 is the excitation rate per pulse and e_2 is the excitation rate per pulse multiplied by the quantum yield of Chlide formation. I$_{675}$* is set within parentheses because it is a short-lived intermediate and, therefore, its concentration at the moment of excitation will be zero. Fitting this model to the data, we obtain the estimated rate constant for each reaction, as indicated in the schemes, 0.045 per pulse for the excitation rate and 0.3 ± 0.1 for the quantum yield (QY) of Chlide formation. The quantum yield of I$_{675}$* product formation in activated enzymes is 0.85, which is obtained from the following expression: $\text{QY} = k_{product}/(k_{product} + k_{loss})$. Here $k_{product}$ and k_{loss} refer to the rates towards the I$_{675}$* state and to the Pchlide*^{II} (or Pchlide*^{III}) state, respectively. The quantum yield for product formation in inactive enzymes is zero. Therefore, in this experiment, by measuring the dynamics on a picosecond timescale and the concentrations of the different populations at time zero, we independently determine the quantum yield of formation of both I$_{675}$* and Chlide formation and find them to be 0.85 and 0.3, respectively.

The estimated difference spectra of the Pchlide*^{I}, Pchlide*^{II} and Pchlide*^{III} states (respectively black, red and blue) are flat in the 670–720-nm region and represent pure Pchlide spectra. The Pchlide*^{III} spectrum most likely represents a fraction of Pchlide not bound to the POR enzyme, whereas the Pchlide*^{I}-to-Pchlide*^{II} dynamic process is probably due to vibrational relaxation. In previous work, we showed that formation of the state emitting at 675 nm depends on the presence of NADPH and the Tyr 189 proton donor[17]. H$^-$ transfer most likely occurs with a rate of $2 \times 10^6\,s^{-1}$ (Supplementary Fig. 1); therefore, we believe that the state emitting at 675 nm is an intermediate in the catalytic reaction and represents the formation of a hydrogen-bonded complex. The spectrum resolved for the I$_{675}$* state (green) shows negative bands at 675 nm and 640 nm, consistent with stimulated emission from I$_{675}$* and bleached absorption of Pchlide. Finally, the spectrum of the state Chlide$_{accum}$* (cyan) is consistent with that of directly excited Chlide, which is formed in previous scans on a timescale longer than nanoseconds, outside the measuring window of the current experiment.

The root-mean-square error of the fit was 0.9×10^{-3}, which means that, with a maximum signal of 26×10^{-3}, the signal-to-noise ratio is almost 30. The matrices of residuals resulting from the target analysis were further analysed using a singular value decomposition[25]. The first left-singular vectors from all seven experiments (Supplementary Fig. 3) show no structure, indicating that all kinetics are described satisfactorily. The structure in the first right-singular vector (Supplementary Fig. 3) resembles the Chlide spectrum, which probably indicates that the noise in the measurement arises from small fluctuations in the transmission of the sample (due to varying relative amounts of Pchlide and Chlide caused by the fact that the movement of the Lissajous scanner is not locked to the acquisition), rather than from noise in the laser pulses.

27. Barth, A. & Zscherp, C. What vibrations tell us about proteins. *Q. Rev. Biophys.* **35**, 369–430 (2002).

28. Iwaki, M., Cotton, N. P., Quirk, P. G., Rich, P. R. & Jackson, J. B. Molecular recognition between protein and nicotinamide dinucleotide in intact, proton-translocating transhydrogenase studied by ATR-FTIR Spectroscopy. *J. Am. Chem. Soc.* **128**, 2621–2629 (2006).

29. Nabedryk, E., Leonhard, M., Mäntele, W. & Breton, J. Fourier transform infrared difference spectroscopy shows no evidence for an enolization of chlorophyll a upon cation formation either in vitro or during P700 photooxidation. *Biochemistry* **29**, 3242–3247 (1990).

30. Hartwich, G., Geskes, C., Scheer, H., Heinze, J. & Maentele, W. Fourier transform infrared spectroscopy of electrogenerated anions and cations of metal-substituted bacteriochlorophyll a. *J. Am. Chem. Soc.* **117**, 7784–7790 (1995).

31. Mäntele, W. G., Wollenweber, A. M., Nabedryk, E. & Breton, J. Infrared spectroelectrochemistry of bacteriochlorophylls and bacteriopheophytins: Implications for the binding of the pigments in the reaction center from photosynthetic bacteria. *Proc. Natl Acad. Sci. USA* **85**, 8468–8472 (1988).